



Neuron-preserving tau coincides with distribution of HSV-1 proteins in Alzheimer's Disease

V.R. Hyde, C. Zhou, K. Chatterjee, J. Fernandez, P. Ramakrishna, A. Lin, G. Fisher, O. Çeliker, J. Caldwell, O. Bender, P. Sauer, P.R. Kinchington⁵, J. Lugo-Martinez⁴, D.Z. Bar³, L. D'Aiuto², and O.A. Shemesh¹ †

1. Department of Neurobiology, 2. Department of Psychiatry, University of Pittsburgh, Pittsburgh, Pennsylvania, 15213 USA 3. The Maurice and Gabriela Goldschleger School of Dental Medicine Research Laboratories, Tel Aviv, Israel 4. Department of Computational Biology, Carnegie Mellon University, Pittsburgh, Pennsylvania, 15213 USA 5. Department of Ophthalmology, University of Pittsburgh, Pittsburgh, Pennsylvania, 15219, USA

Herpes Simplex Virus-1 detected in human Alzheimer's disease brains using metagenomics, mass spectrometry, western blotting, and expansion microscopy; HSV-1 protein expression increases and shifts from neurons to glia with disease severity; HSV-1 colocalizes with phosphorylated tau but not Aβ; HSV-1 infection leads to tau phosphorylation and expression in human derived 3D brain organoids; Specific tau kinase families attenuate ICP27 expression; Phosphorylated tau reduces HSV-1 protein expression and prevents neuronal cell death following HSV-1 infection.

1 HSV-1 detected in human AD brain samples using metagenomics, mass spectrometry & western blots

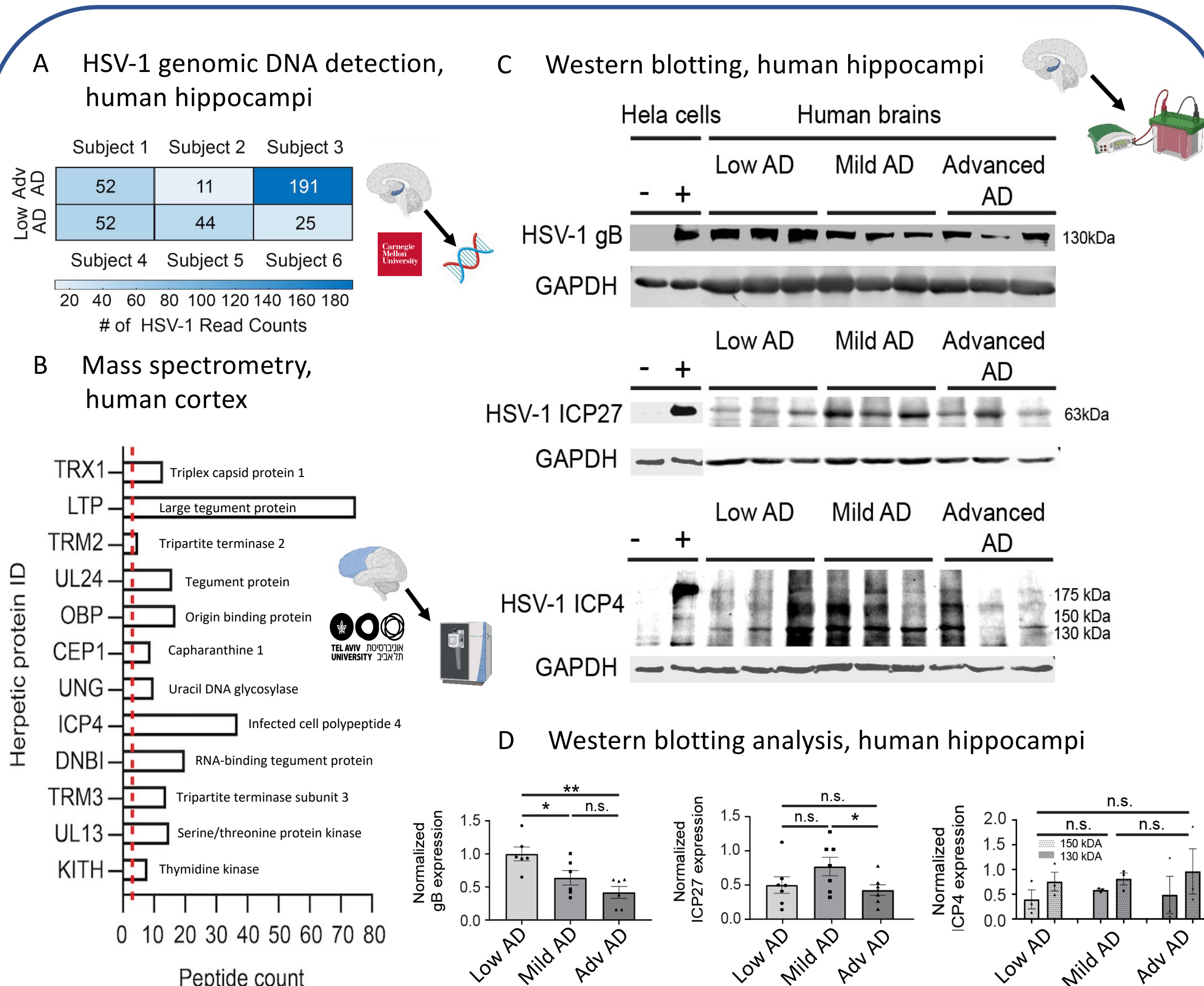


Figure 1. (A) HSV-1 genes were identified using BLAST from metagenomics DNA sequencing data from 6 human hippocampi (3 low AD and 3 advanced AD); total HSV-1 gene counts are shown with respect to the colored scale. (B) HSV-1 proteins were detected in 80 non-AD and AD patient brains using mass spectrometry. (C) HSV-1 proteins were detected in low, mild, and advanced AD brains using western blot and (D) normalized to GAPDH. Data are quantified as mean ± s.e.m. *P < 0.05, **P < 0.01, all other comparisons were found not significant.

7 HSV-1 infection leads to tau phosphorylation and expression in human derived 3D brain organoids

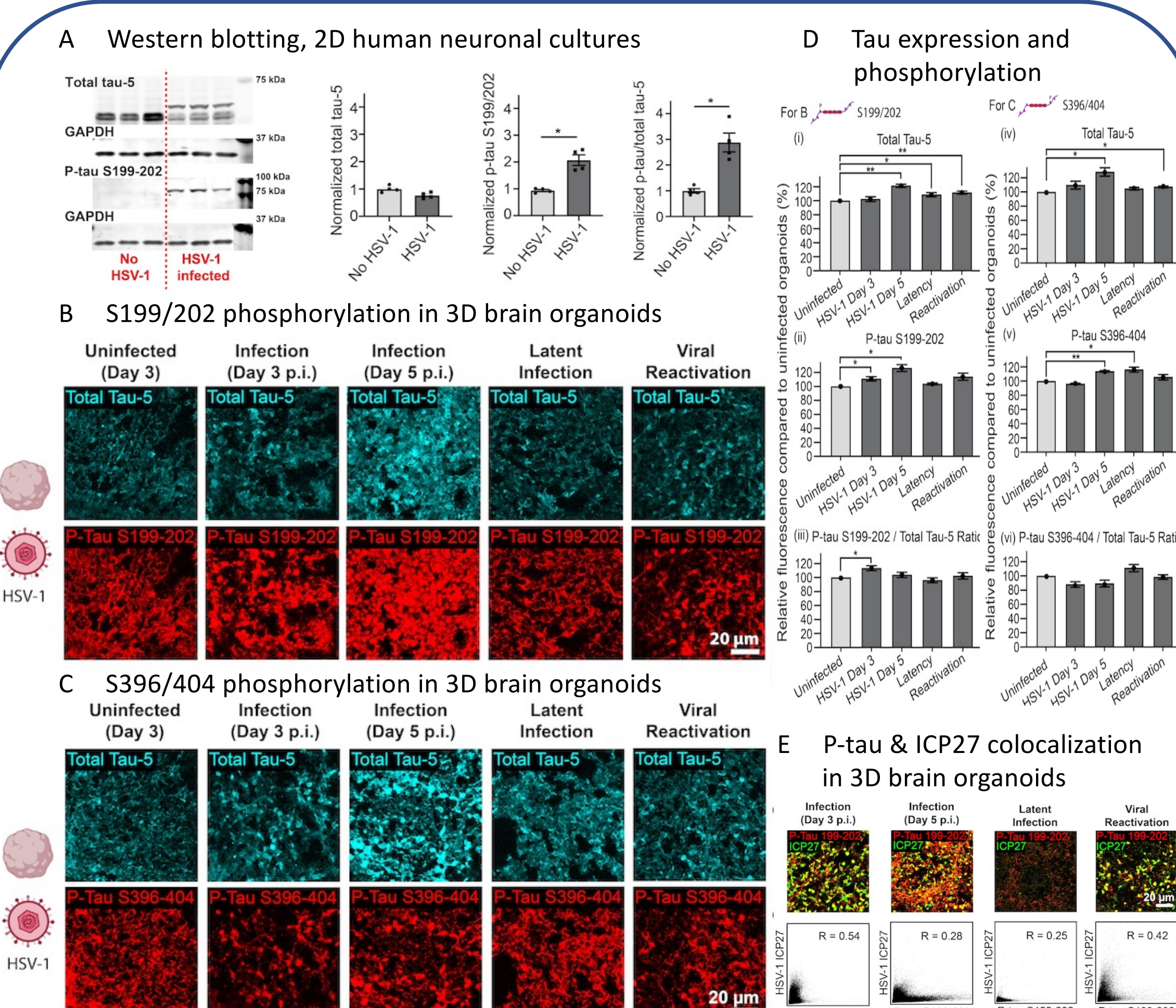


Figure 7. (A) Western blots of tau expression in infected and uninfected 2D human neuronal cultures. (B) S199/202 and (C) S396/404 tau phosphorylation in human derived brain organoids from the following experimental conditions: (a) uninfected, (b) HSV-1 infected organoid, day 3 post-infection (p.i.), (c) HSV-1 infected organoid, day 5 p.i., (d) HSV-1 infected organoid exposed to antiviral 5BVU and INF-α for 7 days (latent infection), or (e) HSV-1 infected organoid exposed to antiviral 7 days, after which the antiviral were withdrawn and infected neurons were exposed to phosphatidylinositol 3-kinase inhibitor for 5 days (viral reactivation); Presented are p-tau in red; total tau in cyan. (D) Bar graphs showing the relative fluorescence of total tau, p-tau, and the tau ratio. (E) Scatterplots showing correlation between p-tau S199/202 and ICP27 with representative images; presented are p-tau S199/202 in red; ICP27 in green. Data are quantified as mean ± s.e.m. *P < 0.05, **P < 0.01, all other comparisons were found not significant.

2 Nanoscale resolution imaging of AD post-mortem samples enabled by expansion microscopy

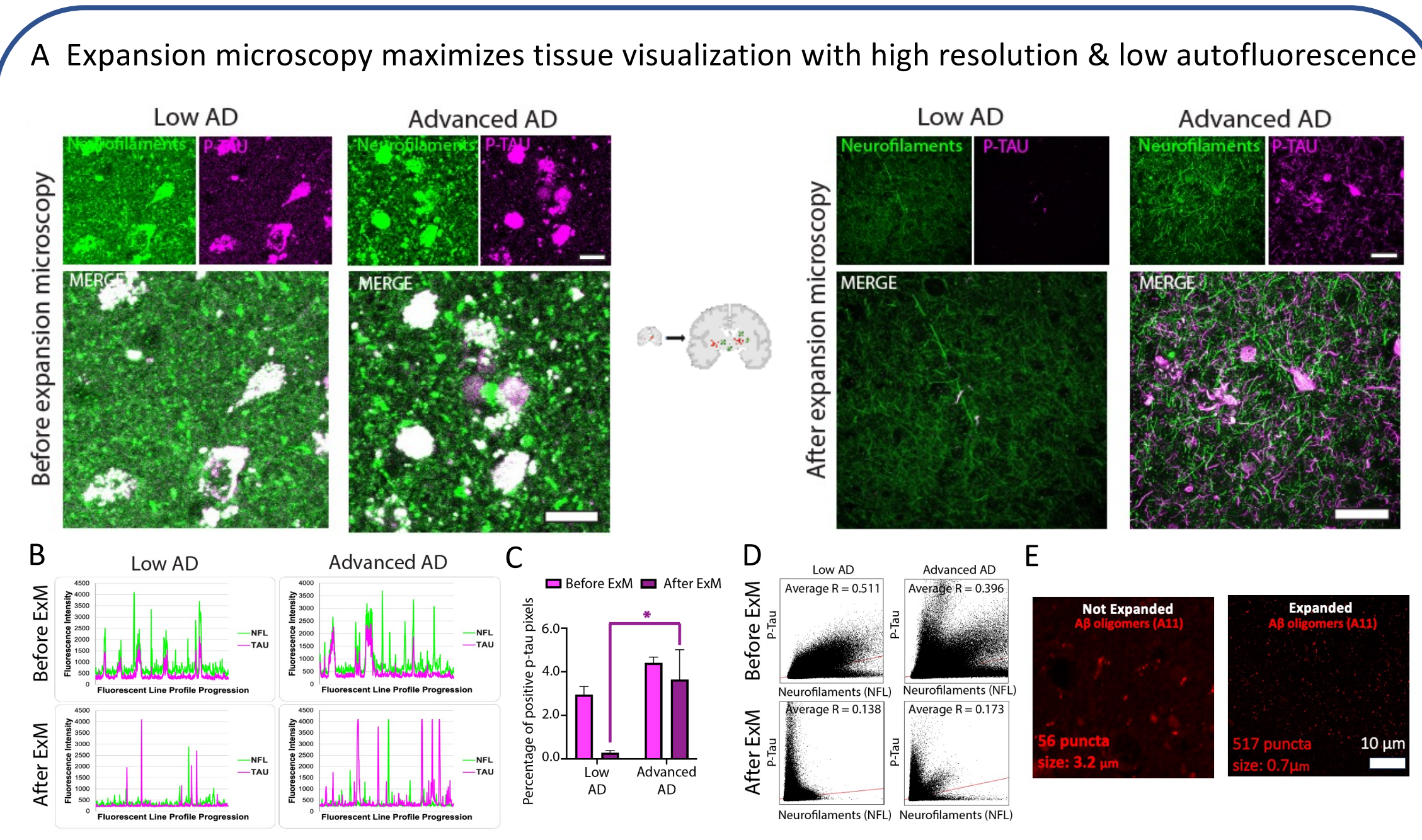
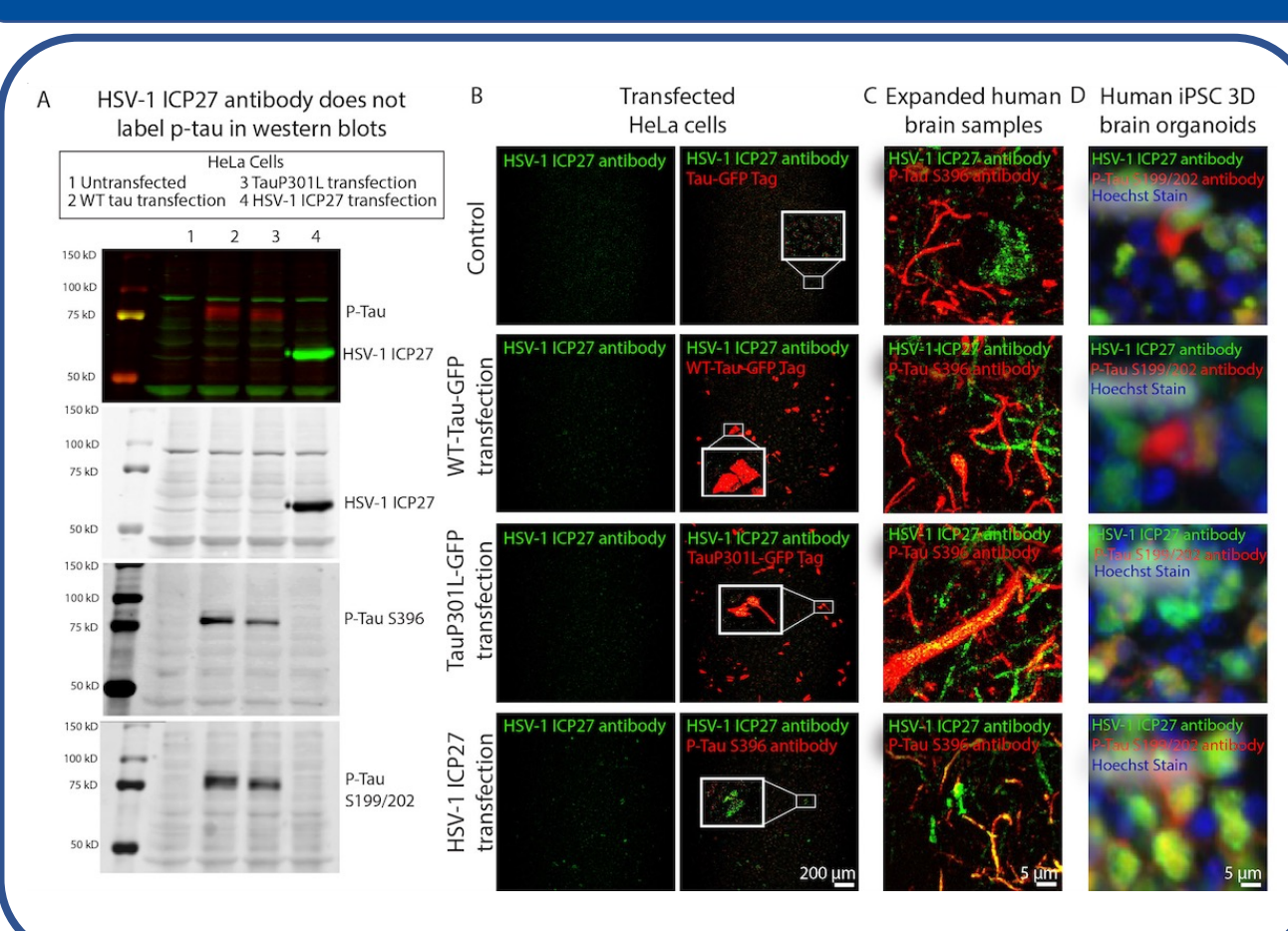
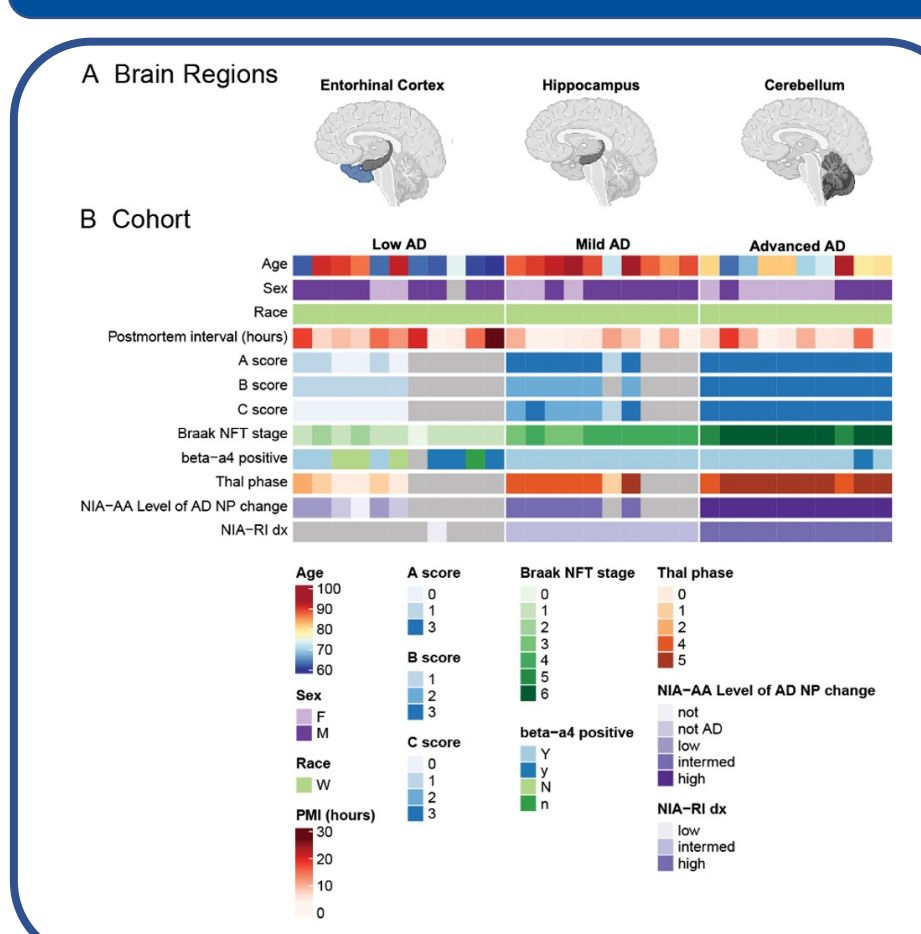


Figure 2. (A) Decrowding expansion pathology (dExPath) increases tissue size by 4.5x, allows for 70nm imaging resolution, eliminates lipofuscin, and exposes previously inaccessible protein epitopes. ExM provides (B) unique fluorescent profiles showing elimination of lipofuscin, (C) predicted significance between tau expression in low vs advanced AD, (D) decreased cross channel colocalization, and (E) increased epitope detection. Data are quantified as mean ± s.e.m. *P < 0.05, all other comparisons were found not significant.

3 P-tau & ICP27 antibody control



4 AD Brain Cohort



5 HSV-1 immediate early proteins increase and shift from neurons to microglia with AD progression

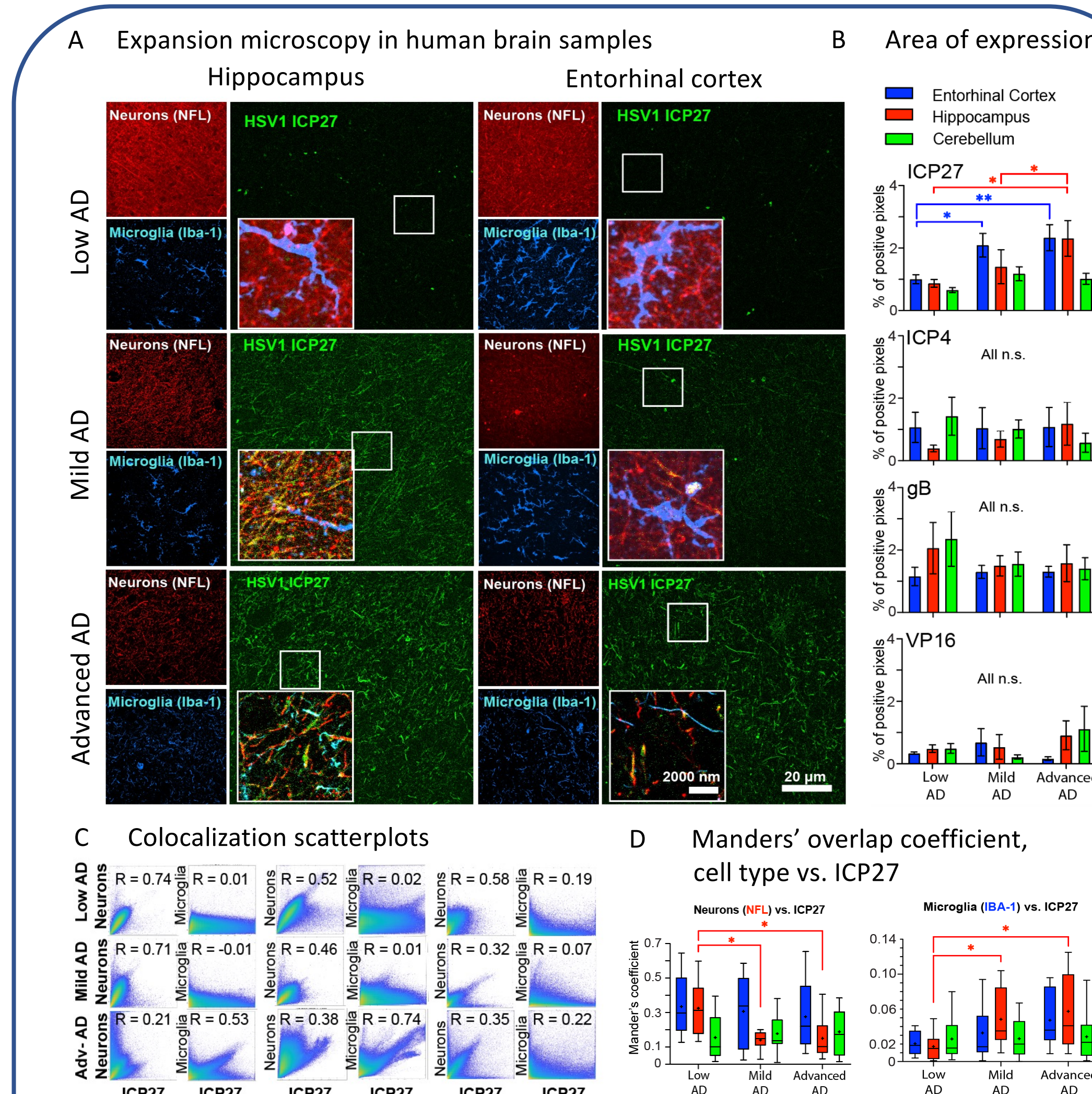


Figure 5. The University of Pittsburgh ADRC provided all the human brains used in this study. (A) Low, mild, and advanced AD brain samples from either the entorhinal cortex, hippocampus or cerebellum were subjected to decrowding expansion pathology and imaged using a confocal microscope, and representative images are shown. For each AD diagnosis and brain area, presented are neurofilaments (NFL) in red; HSV-1 ICP27 in green; microglia (IBA-1) in blue. (B) Bar graphs showing the average percentage of positive pixels for the HSV-1 protein images, for different brain regions and AD diagnoses. (C) Scatterplots showing colocalization between ICP27 and neurons (NFL) or ICP27 and microglia (IBA-1) for different AD diagnoses and brain regions. In each panel, the Pearson's R is given, between the ICP27 image and neuron or microglia image. (D) Box plots showing the Manders' coefficients between cell type (left neuron, right microglia) and ICP27 for low, mild, and advanced AD for the entorhinal cortex (blue), hippocampus (red), and cerebellum (green). *P < 0.05, **P < 0.01, n.s., not significant; all unmarked comparisons were found not significant.

8 Tau phosphorylation in primary neuronal cultures reduces HSV-1 protein expression and preserves neurons

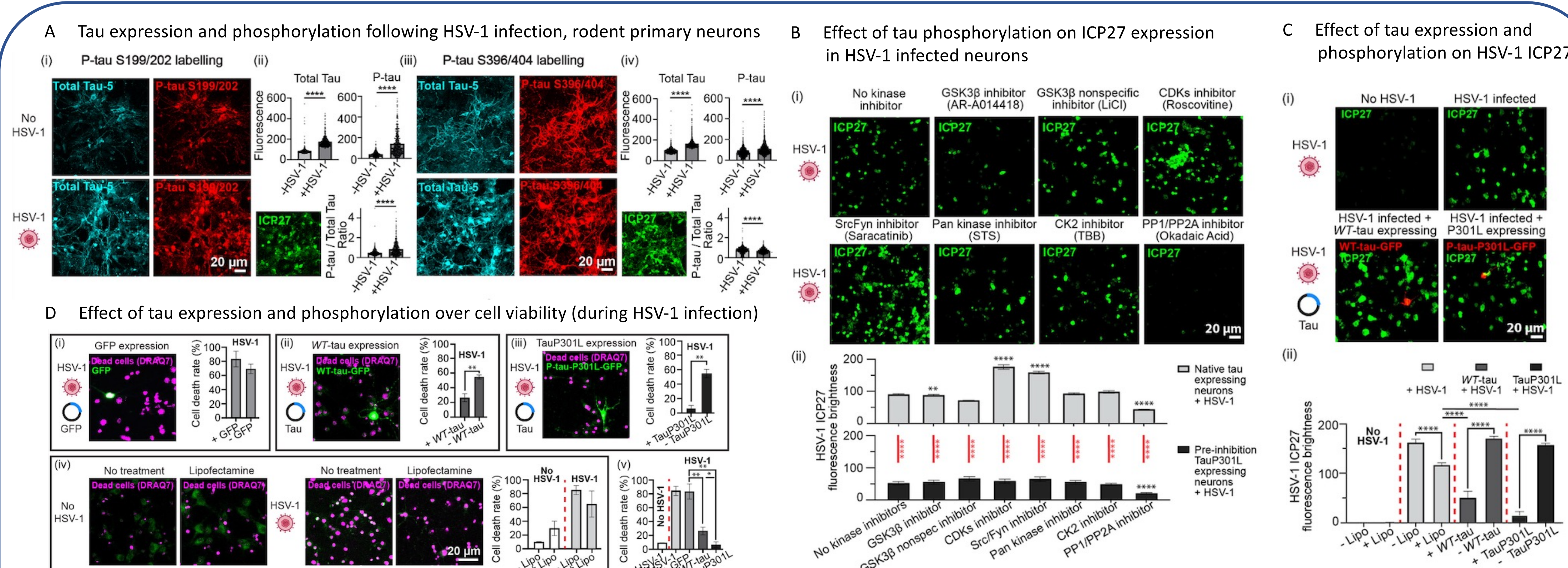


Figure 8. (A) Primary rodent neuronal cultures were infected with HSV-1 (24h) and stained. Presented are total tau in cyan; p-tau in red. Bar graphs showing fluorescence brightness of total tau, p-tau, and the tau ratio. (B) Primary rodent neuronal cultures immersed in various kinase and phosphatase inhibitors were infected with HSV-1 (24h) and stained. Presented are ICP27 in green. Bar graphs showing the ICP27 fluorescence brightness for (top, gray bars) HSV-1 infected neurons exposed to kinase or phosphatase inhibitors or (bottom, black bars) uninfected neurons expressing TauP301L-GFP and exposed to kinase or phosphatase inhibitors. (C) Primary rodent neuronal cultures expressing either WT-tau-GFP or TauP301L-GFP were infected with HSV-1 (24h) and stained. Presented are ICP27 in green; WT-tau-GFP or TauP301L-GFP in red. A bar graph showing the ICP27 fluorescence brightness for both tau expressing neurons and non-expressing neighboring neurons. (D) Primary rodent neuronal cultures expressing GFP, WT-TAU-GFP, or TauP301L-GFP were infected with HSV-1 (24h) and stained. Presented are DRAQ7 death dye in magenta; GFP-tag in green. Bar graphs showing the death rate percentage of the primary rodent cultured neurons. Data are quantified as mean ± s.e.m. *P < 0.05, **P < 0.01, ****P < 0.0001, not all significant comparisons are shown.

6 HSV-1 proteins colocalizes with phosphorylated tau but not with Aβ plaques or oligomers in human brains

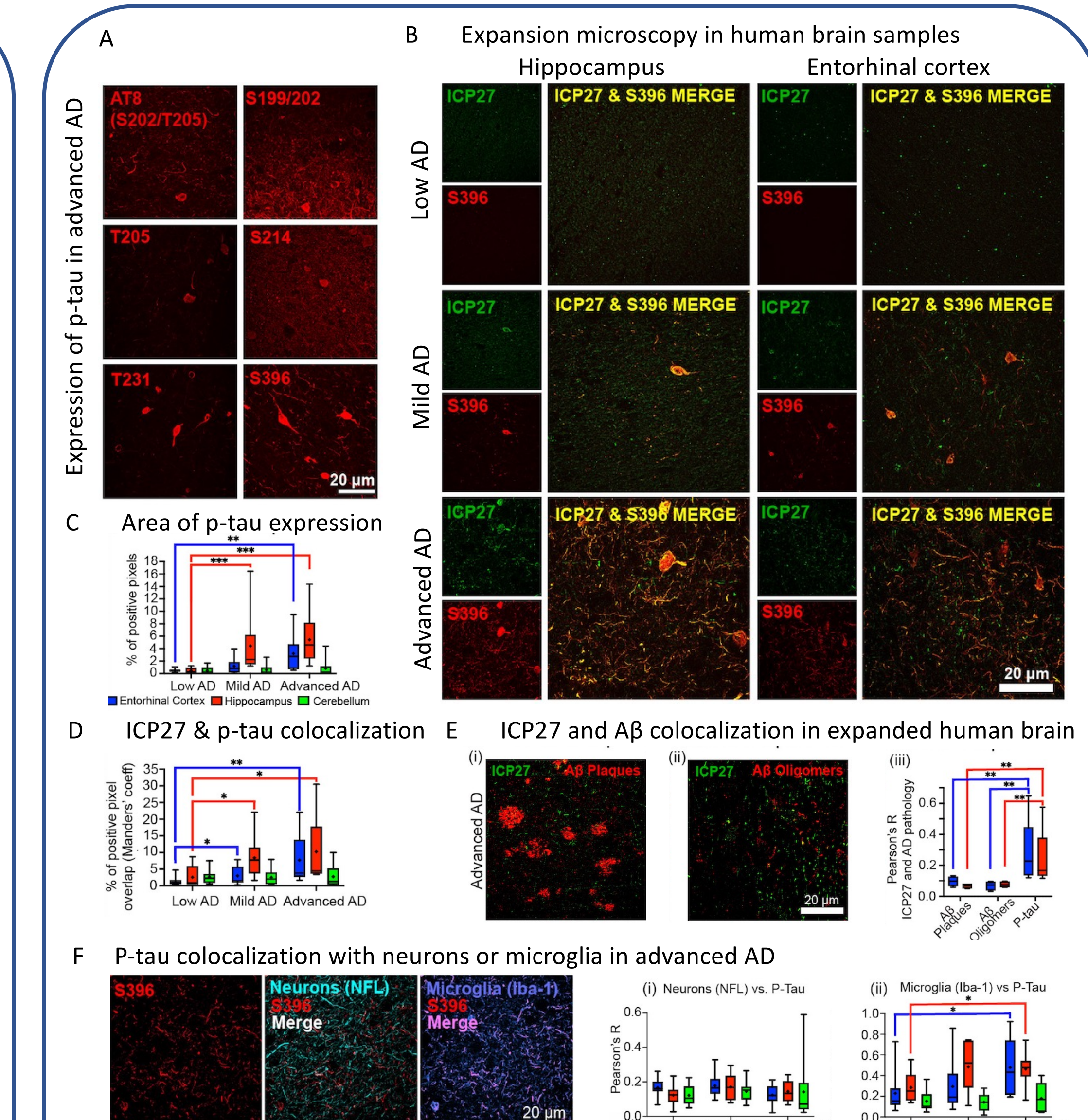


Figure 6. (A) Advanced AD entorhinal cortex were subjected to dExPath and stained with phosphorylated tau sites [AT8 S202/T205, S199/202, T205, T231, S214, S396]. (B) Low, mild, and advanced AD brain samples from either the entorhinal cortex or hippocampus were subjected to dExPath; presented are the ICP27 proteins in green; the p-tau site S396 in red. Box plots showing the (C) area of expression for the p-tau site S396 for different brain regions and AD diagnoses and (D) Manders' coefficients between ICP27 and p-tau site S396. (E) Advanced AD entorhinal cortex were subjected to dExPath; presented are the ICP27 proteins in green; the amyloid beta plaques or oligomers in red. Box plots showing (top) Pearson's R and (bottom) Manders' coefficients between ICP27 and p-tau site S396 or amyloid beta plaques or oligomers. (F) Advanced AD entorhinal cortex were subjected to dExPath; presented are p-tau S396 in red, neurons in cyan, and microglia in periwinkle. Box plots showing Pearson's R between neurons (left) or microglia (right) and ICP27. Data are quantified as mean ± s.e.m. *P < 0.05, **P < 0.01, ***P < 0.001, all other comparisons were found not significant.

Research Summary

Herpes Simplex Virus-1 (HSV-1) DNA and RNA have been previously detected in the human Alzheimer's disease brain; however, viral proteins have never been visualized. Our research shows 19 unique HSV-1 proteins through metagenomics, mass spectrometry, western blots, and expanded human brain samples. These HSV-1 proteins increase with progressive disease severity and shift from neurons to microglia in advanced stages of Alzheimer's disease. These proteins have also been shown to colocalize with hyperphosphorylated tau but not amyloid beta plaques or oligomers. Interestingly, the p-tau can be increasingly found in microglia as patients' approach advanced stages of Alzheimer's disease. In a human derived 3D brain organoid model, HSV-1 infection leads to tau phosphorylation and expression. This change is diminished when HSV-1 latency is established through treatment of antiviral and mildly restored when HSV-1 is reactivated. However, these changes appear to be phosphorylated tau site specific. Similar trends were observed in rodent primary neuronal cultures verifying their use as a model. Using various kinase and phosphatase inhibitors, we found specific tau kinase families to play an important role in ICP27 attenuation. Similarly, expression of native human tau lowered ICP27 expression while expression of mutant human hyperphosphorylated tau almost completely diminished ICP27 expression. Most surprisingly, expression of native human tau reduced cell death while expression of mutant human hyperphosphorylated tau matched uninfected neuronal cultures cell death percentages suggesting that p-tau prevents neuronal death.

Acknowledgements
A huge thank you to the University of Pittsburgh Alzheimer's Disease Research Center (ADRC) for providing brain samples.
Thank you to all our collaborators and mentors for your aid throughout this research journey.
This study was funded by the NIA R56-AG069192-01.

Contact
Or Shemesh
Assistant Professor
Department of Neurobiology
University of Pittsburgh
Email: oshemesh@pitt.edu
orshemesh@gmail.com
Lab Website: shemeshlab.com